

# Sensitivity experiments to mountain representations in spectral models

Antonio Navarra<sup>(1)</sup>, Michela Biasutti<sup>(2)</sup>, Silvio Gualdi<sup>(2)</sup>, Eric Roeckner<sup>(3)</sup>, Uli Schlese<sup>(3)</sup>  
and Uwe Shulzweida<sup>(3)</sup>

<sup>(1)</sup> Istituto Nazionale di Geofisica, Roma, Italy

<sup>(2)</sup> IMGA-CNR, Modena, Italy

<sup>(3)</sup> Max-Planck-Institut für Meteorologie, Hamburg, Germany

## Abstract

This paper describes a set of sensitivity experiments to several formulations of orography. Three sets are considered: a «Standard» orography consisting of an envelope orography produced originally for the ECMWF model, a «Navy» orography directly from the US Navy data and a «Scripps» orography based on the data set originally compiled several years ago at Scripps. The last two are mean orographies which do not use the envelope enhancement. A new filtering technique for handling the problem of Gibbs oscillations in spectral models has been used to produce the «Navy» and «Scripps» orographies, resulting in smoother fields than the «Standard» orography. The sensitivity experiments show that orography is still an important factor in controlling the model performance even in this class of models that use a semi-lagrangian formulation for water vapour, that in principle should be less sensitive to Gibbs oscillations than the Eulerian formulation. The largest impact can be seen in the stationary waves (asymmetric part of the geopotential at 500 mb) where the differences in total height and spatial pattern generate up to 60 m differences, and in the surface fields where the Gibbs removal procedure is successful in alleviating the appearance of unrealistic oscillations over the ocean. These results indicate that Gibbs oscillations also need to be treated in this class of models. The best overall result is obtained using the «Navy» data set, that achieves a good compromise between amplitude of the stationary waves and smoothness of the surface fields.

**Key words** *general circulation – GCM*

## 1. Introduction

The formulation of mountains in the General Circulation Models (GCM) has been one of the first problems to be analyzed in numerical simulation experiments. Mountains are the prime modulator for the structure of the stationary waves in the general circulation. However, they

are far from being an objective, fixed boundary condition. The moderate resolution that is often used in GCMs implies that high resolution data sets for the earth elevation must be degraded and represented with fewer degrees of freedom. The fraction of variability that is not captured explicitly by the resolution of the model must therefore be taken into account via some sort of parametrization process.

In the recent past, various approaches have taken into account hidden variability by enhancing the mean topography in different ways, for example with the «envelope» topography approach of Wallace *et al.* (1983). Even excluding the enhancement algorithms, there is considerable choice between mountain data sets

*Mailing address:* Dr. Antonio Navarra, Dipartimento di Fisica, Settore di Geofisica, Università di Bologna, Viale Carlo Berti Pichat 8, 40127 Bologna, Italy; e-mail: a.navarra@isao.bo.cnr.it

that are all equally valid for representing the topography at moderate resolution. Mountain height at a grid box may be represented by the mean over the box, but such «mean» mountains can differ from each other depending on the particular procedure used for generating and compiling the means. In this paper we analyze the sensitivity of the circulation to two of the most popular data sets in use, the first is derived from the high resolution US Navy elevation data and the second was obtained by a compilation produced at the Scripps Institute (Gates and Nelson, 1975).

Mountains represent a field with strong gradients that are usually poorly represented at intermediate resolution, the inadequacy of the approximation usually shows up most dramatically in spectral models (but grid point models are not exempt, in that case it is simply partially hidden by the numerical dissipation of the schemes) as spurious oscillations of considerable amplitude: Gibbs oscillations.

The problem of Gibbs oscillations is a common complication of using of spectral or pseudospectral techniques in the numerical resolution of differential equations. Spectral techniques have been proven to be very efficient in the resolution of a variety of problems in fluid dynamics, from transonic flow over wing profiles, to combustion simulations. They have been successful even in the case of solutions that include shocks and discontinuities. In climatology and meteorology they have found a wide application as one of the most popular methods for integrating numerically the GCM of the atmosphere.

The most common approach in the treatment of Gibbs oscillations in numerical models of the atmosphere has involved the usage of global or local filters (Hoskins, 1980; Navarra *et al.*, 1994). Global filters are filters whose parameters are independent of position and therefore they can be applied directly to the spectral coefficients, whereas local filters are mathematically a convolution with spatially dependent parameters. Variational methods have also been used to control excess oscillations (Holzer, 1996; Boute-loup, 1995). The two techniques are essentially comparable, especially in the case of local adaptive filters, where the arbitrariness of the choice

of the filter parameters corresponds to the arbitrary choice of the criteria for the cost function in the variational approach.

We present in this paper a local filtering procedure that is based on a mathematical result that allows a very precise control of the filter properties (Gottlieb and Tadmor, 1985). The new idea is that Gibbs waves mark the presence of the discontinuity and in some sense they point to the jump itself. Some recent research has developed a method that recovers a better approximation to the original data from the Fourier coefficients themselves. The technique (Gottlieb and Tadmor, 1985, in the following GT) is based on the construction of a regularization kernel (the «Dirichlet filter») that yields an approximation that is spectrally precise. The construction of the kernel is heuristic and it must be developed case by case. In the case of the topographies discussed in this paper it has been possible to construct a working function that has effectively eliminated Gibbs oscillations over the ocean and over land.

The first objective of this paper is to give an appreciation of the sensitivity of the response to the specification of mountains and secondly to illustrate the performance of the Dirichlet filter in the spectral model. Gibbs oscillations seem to be able to influence the surface energy budget via modulation of the evaporation and, to a lesser degree, the precipitation field. The filtered topography generally improves the surface fields by reducing the amount of spurious oscillations. The filter also impacts the upper air field by reducing the systematic error in the stationary waves over Europe, with respect to Standard mountains. The sensitivity to the particular mountain data is distinctive, showing that the stationary waves can be modified rather substantially by small modifications in the mountain field.

## 2. The construction of the kernel

The procedure for the construction is described in detail in GT. We will briefly sketch here the major points, in GT the results were obtained for the time evolution of a set of hyperbolic equations, but we will consider here only



the case at fixed time. The starting point in the procedure is a theorem that extends Greens relation, basically proving that if  $u(x)$  and  $u_N(x)$  are a function and its spectral approximate, than the following relation holds for any smooth (infinitely differentiable) function  $v$

$$\langle u_N | v \rangle = \langle u | v \rangle + \varepsilon. \quad (2.1)$$

where  $\varepsilon$  is exponentially small (namely goes to zero faster than any power),  $\langle \dots | \dots \rangle$  indicates a scalar product. This relation means that  $u_N(x)$  approximates  $u(x)$  weakly: in this sense  $u_N(x)$  contains accurate information about  $u(x)$ . The result in eq. (2.1) can be cast in the following form in the case that  $u_N(x)$  is obtained via a pseudospectral method:

$$\frac{\pi}{N} \sum_{j=0}^{2N-1} u_N(x_j) v(x_j) = \int_0^{2\pi} u(x) v(x) dx + \varepsilon \quad (2.2)$$

where  $N$  is the truncation of the pseudospectral method evaluated at points  $x_j$  and  $\varepsilon$  is exponentially small. The problem with the spectral sum is that  $u_N(x)$  converges to  $u(x)$  in a square norm sense, but not uniformly. The convergence may fail in a limited number of points, usually the points of discontinuity. We can use eqs. (2.1) and (2.2) to obtain a better approximation to the original function near the discontinuity than the evaluation of  $u_N(x_j)$  by noting that such an approximation  $u_N(y)$  to in some point  $y$  can be obtained by finding a function  $v_y(x)$  such that

$$u(y) + \varepsilon_1 = \int_0^{2\pi} u(x) v_y(x) dx. \quad (2.3)$$

Using eq. (2.2) we will also have

$$\frac{\pi}{N} \sum_{j=0}^{2N-1} u_N(x_j) v_y(x_j) = u(y) \varepsilon_1 + \varepsilon \quad (2.4)$$

for the pseudospectral method.

The function  $v_y(x)$  was constructed following the indications in GT. It consists basically of the Dirichlet kernel of the Fourier transform multi-

plied by a highly localized function. GT suggested

$$v_y = \frac{1}{\theta} \rho_\alpha \left( \frac{y}{\theta} \right) D_p \left( \frac{y}{\theta} \right)$$

$$D_p \left( \frac{y}{\theta} \right) = \frac{1}{2\pi} \sum_{|k| \leq p} e^{ikx} = \frac{1}{2\pi} \frac{\sin((p+1/2)y/\theta)}{\sin(y/(2\theta))}$$

$$\rho_\alpha = \begin{cases} \exp\left(\frac{\alpha \xi^2}{\xi^2 - 1}\right) & |\xi| < 1 \\ 0 & |\xi| \geq 1 \end{cases} \quad (2.5)$$

where  $D_p$  is the Dirichlet kernel for the finite Fourier transform truncated at wavenumber  $p$ .

The preceding theorems and definitions hold only for the case of the Fourier transform. The extension to spherical harmonics will require writing down the kernel of the Legendre polynomial transformation in closed form and demonstrate that a function like  $v_y(x)$  exists. It is important, before proceeding to such an extension, to assess if there is any impact even in a partial removal of Gibbs oscillations, *e.g.*, applying it only to the zonal direction. It will be apparent in the following section that a large portion of Gibbs error is, in fact, associated with the zonal direction.

«Standard» orography is the data set used in all ECHAM models, originally prepared at ECMWF. This data set is based on the Navy data, but it has been enhanced by an envelope orography and then smoothed by a Gaussian filter.

The «Navy» and «Scripps» data sets prepared for the sensitivity experiments have been transformed onto the same Gaussian grid by area averaging. The «Navy» data set used in this paper is the high resolution US Navy data at 10' resolution (Joseph, 1980). The «Scripps» data set (Gates and Nelson, 1975) is at 1 degree resolution. The Standard, Navy and Scripps topographies are shown in fig. 1 for the Northern Hemisphere. The comparison indicates (with the help also of the bottom panels of figs. 21 and 23) the large scale patterns are broadly similar, the altitude of the main mountain sys-

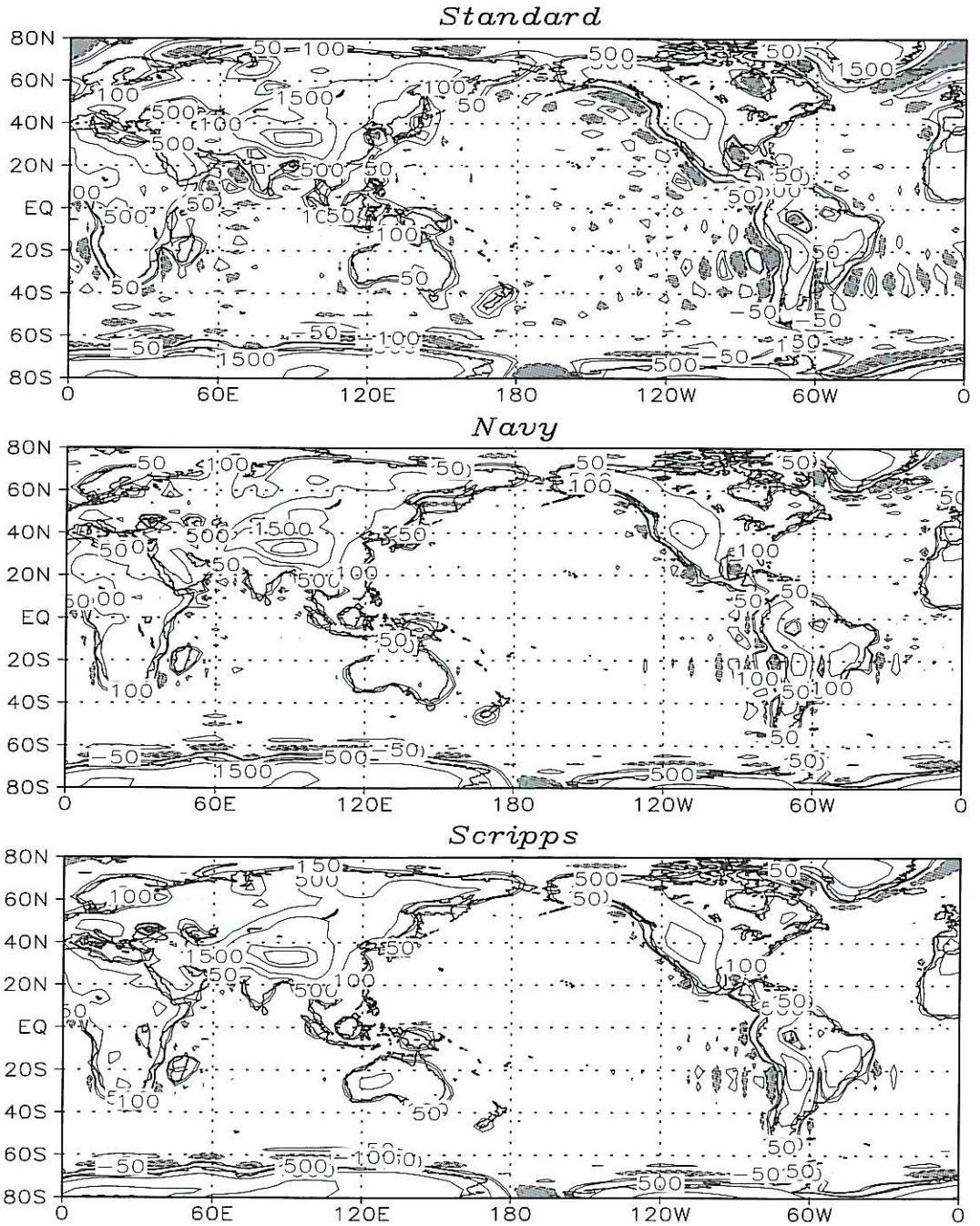


**Fig. 1.** Northern Hemisphere topographies for the Standard, Navy and Scripps case. The contours are at 4500, 3500, 1500, 500, 100, 50, -50, -100, -300, -50 m.



tems is comparable. The «Navy» and «Scripps» sets display a substantial reduction in Gibbs oscillations over the oceans (obviously zero in the original data set). There are differences also in the smaller features over the continents, but we cannot attribute these features to the Gibbs oscillations entirely in this case, since small-scale differences between the data sets come into play. The differences tend to be more uniform over the continents for the Scripps case, whereas in the Navy case they are less organized. The continental differences are, however, limited, of the order of 200-300 m.l.

### 3. The Dirichlet filter applied to the earth elevation

The Dirichlet filter performance will be illustrated in the case of Navy topography, the results in the case of the Scripps data are essentially similar. The first choice was to decide which is a fair set of observations to use as a comparison for the spectral topography, filtered and unfiltered. The 30 waves in the longitudinal direction of a T30 can at most represent 60 points, it seems unfair to verify against observation with a much higher number of points. The original high-resolution data sets were therefore interpolated to an «optimal» grid for the T30 ( $60 \times 48$ ) that represent the largest content of information that can be stacked into the Fourier part of a T30 truncation. The target is to produce topographies on the Gaussian grid of  $96 \times 48$  that is used in the GCM, but the comparison is done with respect to the «optimal» grid.

The figures show the result of the application of the Dirichlet filter on a topography data set, in this case the Navy data set. Figure 2 shows the Eastern Pacific area, the bottom panel illustrates the target data interpolated to the «optimal» grid for a T30 spectral model ( $60 \times 48$  Gaussian). This grid is only partially optimal because it represents good collocation points only for the longitudinal part of the spectral transform, the Fourier transform in longitude. In the case of the Pacific, however, the Gibbs error of the Fourier component is dominant, as can be seen from the top panel that shows the unfiltered «Standard» orography. Gibbs wave-

trains develop primarily in the east-west direction into the Pacific Ocean. The other data sets, that include the filtering procedure, show a reduced oscillation. The details of the filtering procedure, including codes, are available on request from the authors.

The exploration of the parametric space of the Dirichlet filter shows little sensitivity to the values of  $\alpha$ , but a large dependence on the values of  $\theta$ . The filter is a compact support function and it is reasonable that the diameter of the support ( $\theta$ ) influences the action of the kernel more than the rate of decrease inside the support ( $\alpha$ ). The following calculations have been performed with a value of  $\theta = 1.25$ , but smaller values have been used approaching the Andes region from the Pacific Ocean to make sure that the interval does not include the discontinuity. It is interesting to note that the Dirichlet approach produces little damage to the gradient. The filtered field is less stretched than a standard transform and the coastal topography gradient is better represented. We are exploiting here the freedom provided by the Dirichlet filter and the kernel is adjusted to be narrower and narrower as it nears the coast to reduce damage to the amplitude and to the gradient. The adjustment is realized by using smaller values of  $\theta$  in eq. (2.5) for the grid points closer to the Andes, resulting in a sharper kernel and in a better definition of the jump at the Andes.

Another important area where topography is supposed to play an important role in the control of climate variability is the Indian Ocean sector (fig. 3). Numerical studies have indicated that Gibbs oscillation can play a role in the simulation of the Indian monsoon (Fennessy *et al.*, 1994). In contrast with the Pacific case, it is not obvious here that the source of Gibbs error is in the Fourier transform, because of the complex geographical distribution of the mountains. Nevertheless, the Dirichlet filter successfully removes all the undulations in the Indian Ocean and the big dips in the Ganges plain. There is a small overshoot of the Himalayan peaks in a limited region, but overall the fit is very good. Another example of the behavior of the filter in land regions is illustrated by the following picture, the Rocky mountain area (fig. 4). In this case the usual oceanic oscillations are eliminat-

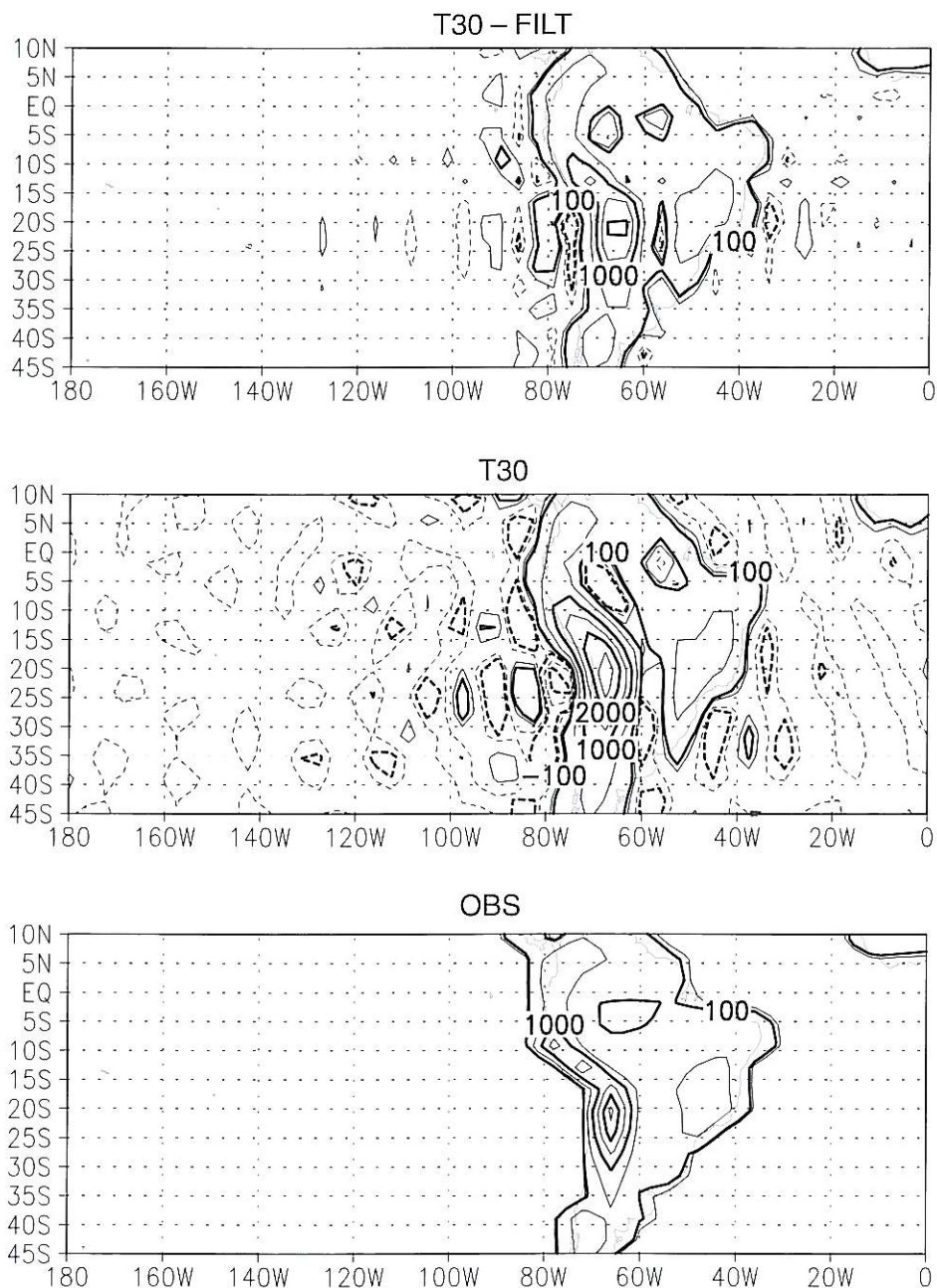


**Fig. 2.** Mountains representation for the T30 spectral model. Bottom panel, target data obtained from the Navy high resolution data set, middle panel standard T30 spectral transform, top panel, the field after the Dirichlet filter with parameters discussed in Section 2. Contours are at  $-500$ ,  $-300$ ,  $-100$ ,  $-50$ ,  $50$ ,  $100$ ,  $500$  m and every  $1000$  m after elevations of  $1000$  m. Negative contours are dashed.



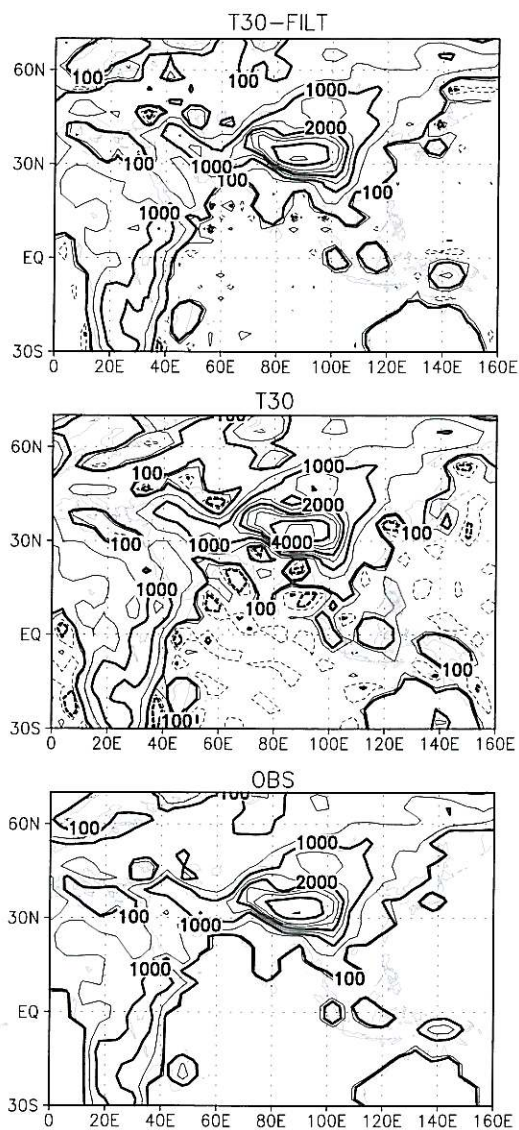


Fig. 3. As in fig. 2 but for the Indian sector.

ed, but the excess amplitude over the Rockies introduced by the spectral transform (Gibbs error on land) is also successfully eliminated by the Dirichlet filter.

The last example I of this section is in the Antarctic continent (fig. 5) and it shows that the

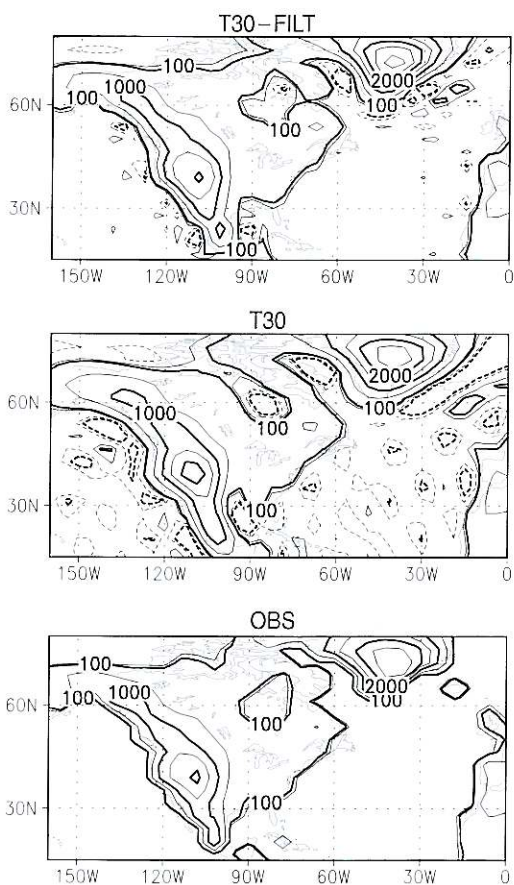
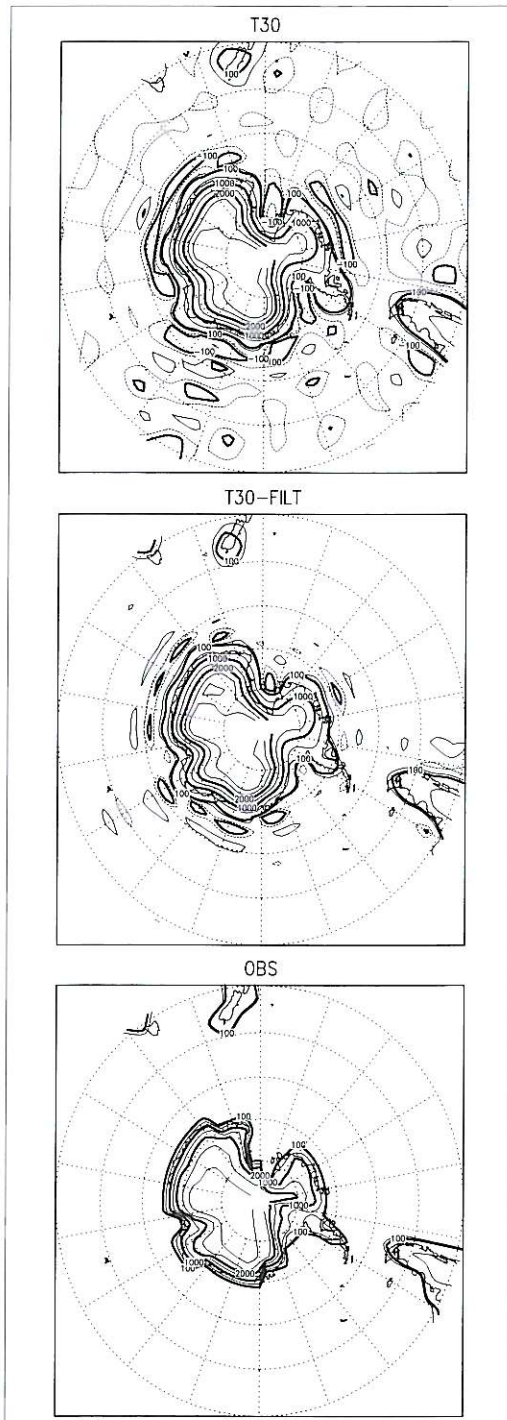


Fig. 4. As in fig. 2 but for North America.

Dirichlet filter recovers the right distribution, but the efficiency of the recovery is more limited in this case since Gibbs oscillations are generated by the meridional direction, *i.e.* the Legendre part of the transform.

It is possible to note that the new filter realizes a good fit to the target data in fig. 6, showing a section along 20S in the Pacific Ocean. In this picture we plotted the observation data, the unfiltered spectral data and mountains filtered with the Dirichlet filter and with a simple exponential filter (Hoskins, 1980). The filter has an exponential form ( $\exp^{-32m/N^6}$ ) designed to strongly dump the wavenumbers close to the total wavenumber  $N_{MAX}$ . The Dirichlet filter is mitigating



the oscillations in the marine area, eliminating the big dip of 500 m right off the coast of Peru. It also improves the representation of the gradient right at the coast, resulting in an improved sharpness of the profile. The entire Andes profile needed three gridpoints in the standard T30, whereas the new method requires only two points. A similar situation can be observed for the Rocky Mountains (fig. 7). Also in this case the fit is improved by the Dirichlet filter.

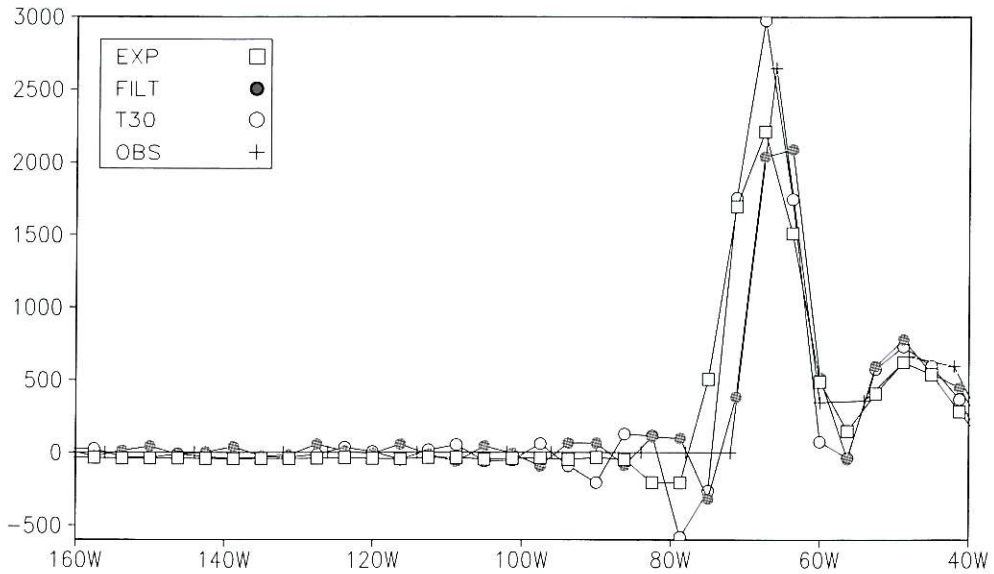
The procedure was applied only to the longitudinal transforms, but it has had an impact on the quality of the fit at the collocation point overall. A section along the 90E meridian shows considerable improvement in the Indian sector (fig. 8). The Dirichlet filtered topography follows the data better, whereas the exponential filter appear to be excessively smoothing. The overall reduction of the oscillation can be measured with the root mean square difference with the observations (table I). The oscillations are moderately reduced globally, but larger reductions can be noticed in the Andes and Indian regions corresponding to the sections shown in the preceding pictures. A further illustration of the effect of the filtering procedure can be given by showing the spectral plots of the spherical harmonics coefficients (fig. 9). The filter removes the slow decay at high wavenumbers, but it leaves the wavenumbers 1-10 substantially untouched. The slow decay with growing wavenumber is a typical sign of Gibbs effect, as it can be seen from fig. 10, that shows the modulus of the spherical harmonic coefficients averaged over the meridional wavenumbers.

#### 4. Numerical experiments

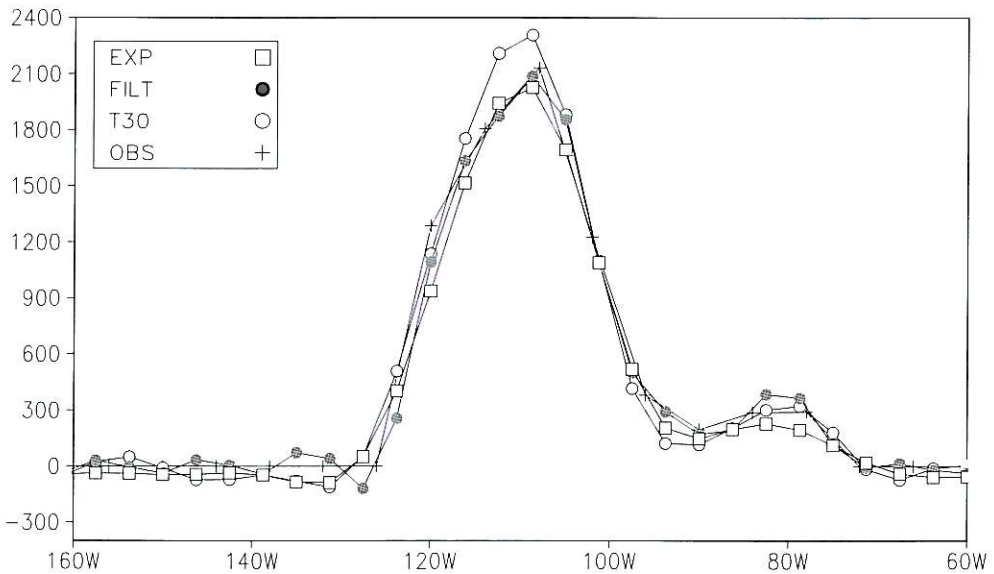
The numerical experiments consist of three 10 year simulations, a control AMIP integration from 1979 to 1988, a «Navy» experiment with the filters topography based on the Navy data, a «Scripps» experiment with the filtered topography based on the Scripps data. All simulations

Fig. 5. As in fig. 2 but for the Antarctica.





**Fig. 6.** Section along 20S for the topographies from the Navy data. Observations are indicated by crosses, the exponential filter by an open square, a standard T30 spectral topography is indicated by open circle and the Dirichlet filter by filled circles. The gradient between the Andes and the Pacific Ocean is better represented in the Dirichlet filter case.



**Fig. 7.** Section along 40N for the topographies from the Navy data. Observations are indicated by crosses, the exponential filter by an open square, a standard T30 spectral topography is indicated by open circle and the Dirichlet filter by filled circles.

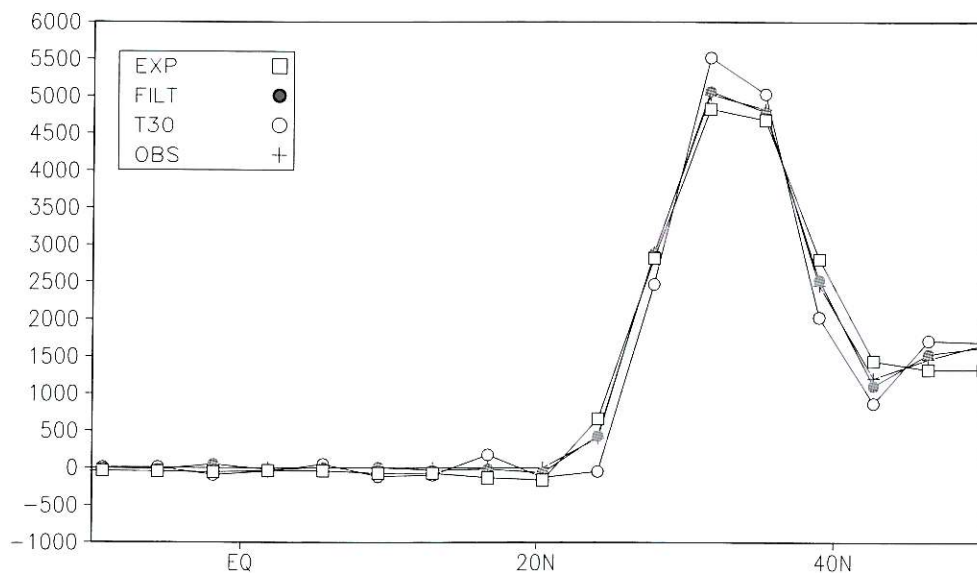


**Fig. 8.** Section along 90E for the topographies from the Navy data. Observations are indicated by crosses, the exponential filter by an open square, a standard T30 spectral topography is indicated by open circle and the Dirichlet filter by filled circles.

**Table I.** Root mean square difference from the observation for filtered and unfiltered orographies shown in the preceding sections and for the entire globe.

	Global	Andes	India
Unfiltered	4.63	2.10	1.07
Filtered	3.89	0.90	0.19

use the same initial condition for arbitrary conditions corresponding to Northern Hemisphere winter. The first year was discarded and the remaining 9 years have been used in the analysis. The observations are based on the ECMWF analyses for the period 1980-1987 as compiled by Schubert *et al.* (1990). The integrations were performed with the ECHAM4 T30 model (Roeckner *et al.*, 1996). In the following the terms «winter» and «summer» refer to Northern Hemisphere winter and summer, respectively.

#### 4.1. Upper air circulation

The impact on the upper air flow is shown in fig. 11. The 200 mb zonal flow is not strongly affected by the differences in the mountain representation, either in winter or summer. There are minor differences in the strength and position of the jet, but overall there is no strong sensitivity. The summer situation (not shown) reveals a similar behavior. The meridional velocity field (fig. 12), instead, is strongly affected by the mountains. The velocity field in the standard experiment is too strong over the European region, with values in excess of 12 m/s. Navy orography improves the situation reducing the error over Europe, whereas Scripps orography produces velocities that are still too intense in the European and American sectors.

The response of the upper air flow can be seen more easily in fig. 13 that shows the eddy (deviation from the zonal mean) component of the geopotential at 500 mb. The Standard experiment has a good overall structure of the stationary waves, but the positive anomaly over Eu-



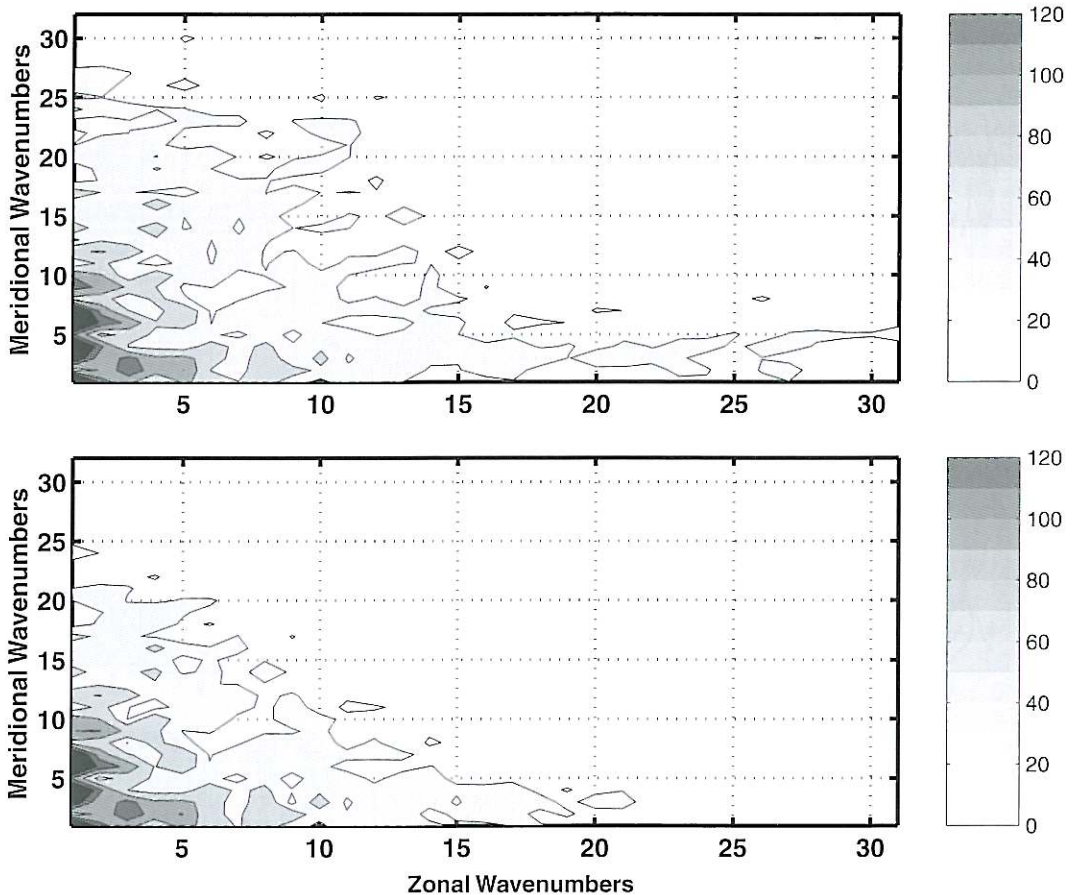


Fig. 9. Absolute value of the spectral coefficients for the unfiltered (top) and filtered (bottom) «Navy» orography, in meters.

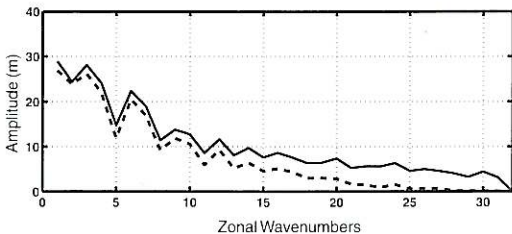
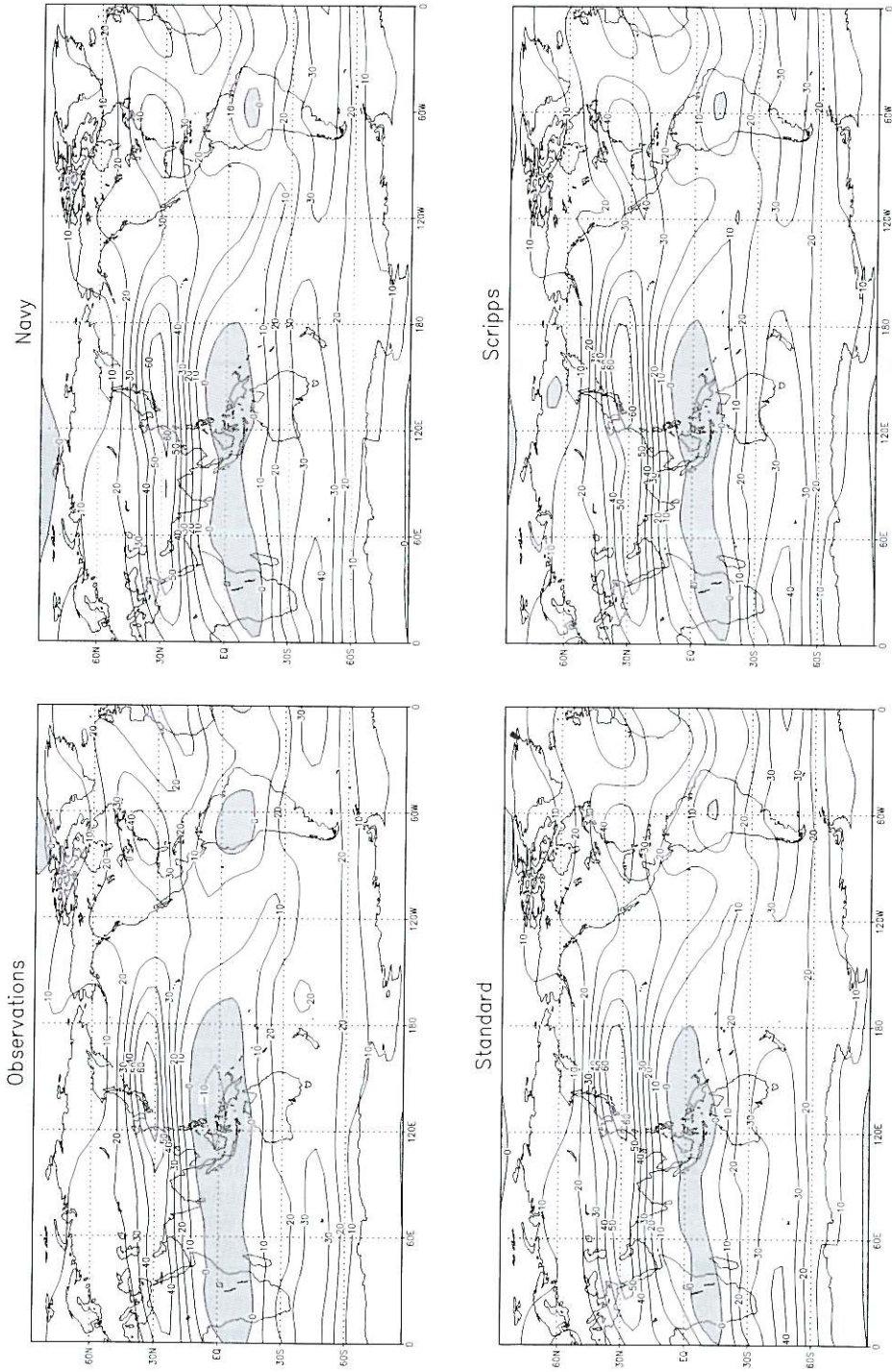


Fig. 10. Average of the modulus of the spherical harmonics coefficients over the meridional wavenumbers. It is possible to notice the very slow decline of the unfiltered coefficients (solid line). The filtered fields drop more rapidly (dashed line).

rope tends to be too strong, whereas the negative anomaly over Canada tends to be weaker. The string of subtropical anomalies tend to be of larger amplitude than observed. The shape of the European anomaly is also somewhat insufficient because the tongue of anomalies does not push into the Asian continent as observed. Overall, the Navy mountains seem to give the best tradeoff between reducing the excess amplitude over Europe and limiting the reduction of the positive center over the Gulf of Alaska.

The Navy filtered mountains (top right) show a strong reduction in amplitude of the wavetrains over Europe and a change in shape of the anoma-



**Fig. 11.** Winter (DJF) zonal flow at 200 mb for the observations (OBS), the Standard experiment, the Navy mountains data set and the Scripps mountains. The simulation of the winter zonal mean is largely unaffected by the orographic data. Negative values are shaded. The contour is 10 m/s.



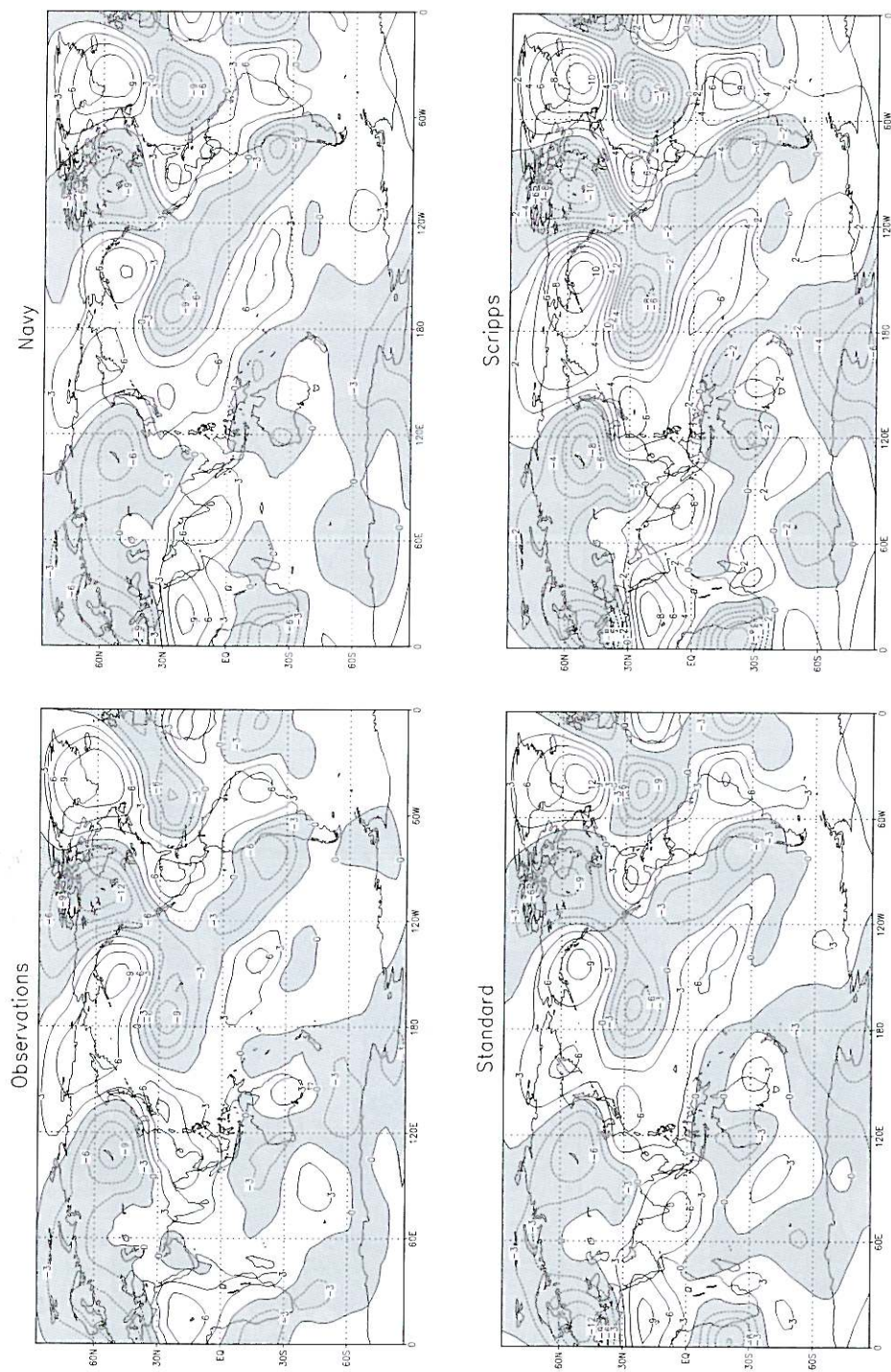


**Fig. 12.** Winter (DJF) meridional flow at 200 mb for the observations (OBS), the Standard experiment, the Navy mountains data set and the Scripps mountains. Negative values are shaded. The contour is 3 m/s.